HHS Public Access

Author manuscript

J Neurooncol. Author manuscript; available in PMC 2016 September 01.

Published in final edited form as:

J Neurooncol. 2015 September ; 124(3): 365–372. doi:10.1007/s11060-015-1853-7.

VB-111: A novel anti-vascular therapeutic for glioblastoma multiforme

Aleksandra Gruslova[1], **David A Cavazos**[1], **Jessica R. Miller**[1], **Eyal Breitbart**[2], **Yael C Cohen**[2], **Livnat Bangio**[2], **Niva Yakov**[2], **Anu Soundararajan**[1], **John R. Floyd**[1], and **Andrew J. Brenner**[1]

[1]Cancer Therapy and Research Center, Department of Radiology, The University of Texas Health Science Center at San Antonio, 7703 Floyd Curl Drive, San Antonio, Texas 78229-3900

[2]VBL Therapeutics, 6 Jonathan Netanyahu St., Or Yehuda, Israel 60376

Abstract

Glioblastoma multiforme (GBM) is among the most highly vascularized of solid tumors, contributing to the infiltrative nature of the disease, and conferring poor outcome. Due to the critical dependency of GBM on growth of new endothelial vasculature, we evaluated the preclinical activity of a novel adenoviral gene therapy that targets the endothelium within newly formed blood vessels for apoptosis. VB-111, currently in phase II clinical trials, consists of a non-replicating Adenovirus 5 (El deleted) carrying a proapoptotic human Fas-chimera (transgene) under the control of a modified murine promoter (PPE-1-3x) which specifically targets endothelial cells within the tumor vasculature. Here we report that a single intravenous dose of 2.5×10^{11} or 1×10^{11} VPs was sufficient to extend survival in nude rats bearing U87MG-luc2 or nude mice bearing U251-luc, respectively. Bioluminescence imaging of nude rats showed that VB-111 effectively inhibited tumor growth within four weeks of treatment. This was confirmed in a select group of animals by MRI. In our mouse model we observed that 3 of 10 nude mice treated with VB-111 completely lost U251 luciferase signal and were considered long term survivors. To assess the antiangiogenic effects of VB-111, we evaluated the tumor-associated microvaculature by CD31, a common marker of neovascularization, and found a significant decrease in the microvessel density by IHC. We further assessed the neovasculature by confocal microscopy and found that VB-111 inhibits vascular density in two separate mouse models bearing U251-RFP xenografts. Collectively, this study supports the clinical development of VB-111 as a treatment for GBM.

Keywords

Glioblastoma; VB-111; angiogenesis; gene therapy; tumor vasculature

Corresponding Author: Andrew J. Brenner, Telephone: 210-450-5936, Fax: 210-692-7502, brennera@uthscsa.edu.

Conflict of Interest Statement: A. B. received a commercial research grant from and is a consultant/advisory board member of Vascular Biogenics. Y.C.C., L.B., N. Y. and E. B. are employed by and have ownership interest in VBL Therapeutics.

Introduction

Glioblastoma (GBM, WHO grade IV) is the most common and aggressive of the primary brain tumors in adults, with poor prognosis despite intervention with surgery, radiation and chemotherapy. Annually, 5 in 100,000 people are diagnosed with GBM, with a median survival of approximately 14 months [1]. The low survival is attributed partly to the nature of the tumor. GBMs are highly vascularized tumors and display markedly disorganized vascular structures with conspicuous endothelial cell proliferation, pericyte and basement membrane abnormalities resulting in permeability with heterogeneous leakiness and abnormal blood flow [2]. The location of the tumor also makes drug delivery difficult with only small or lipophilic molecules able to cross the blood brain barrier [3, 4]. Of those agents that are able to reach the tumor, GBMs have shown to be resistant to most cytotoxic agents and quickly develop resistance when initially sensitive [5, 6].

Antiangiogenic therapy has rapidly evolved into an integral component of standard therapy for many malignancies. As an example, bevacizumab, a humanized monoclonal antibody against vascular endothelial growth factor (VEGF), was the first antiangiogenic drug to receive approval and is now considered a component of standard of care for ovarian, lung, kidney, colon and brain cancers [7–12]. Yet, while antiangiogenics have improved the practice of clinical oncology, clinical outcomes suggest that these therapuetics only prolong overall survival of cancer patients by several months, without offering enduring cure [13, 14]. This may be in part due to tumor cells evading angiogenic inhibitors through modulation of collateral pathways or due to co-option of existing normal vasculature to maintain adequate blood perfusion. To overcome the limitations of existing antiangiogenic drug therapies, which ultimately fail, we assessed the efficacy of using VB-111 to target newly formed blood vessels. VB-111 is a nonreplicating adenovirus 5 (Ad-5, El-deleted) carrying a proapoptotic human Fas-chimera transgene (Fas and human TNF receptor 1) under the control of a modified murine pre-proendothelin promoter (PPE-1-3x) [15–17]. This modified murine promoter is able to specifically target the expression of the Fas-chimera transgene to angiogenic blood vessels, leading to targeted apoptosis of these vessels (Fig. 1). Because the transgene specifically targets the endothelial cells on the luminal wall of the neovasculature, penetration through the blood brain barrier is not required.

We have recently published a phase I, open-label, multisite, sequential dose-escalation clinical trial with a single dose of VB-111 (NCT00559117) showing that VB-111 is safe and well tolerated in patients with advanced metastatic cancer at a single infusion of up to 1×10^{13} viral particles (VPs), with evidence of transgene expression in tumor tissue and tumor responses observed [18]. In addition, a phase II open-label multicenter study is being conducted to determine the efficacy of VB-111 in treating patients with GBM (NCT01260506). Here we confirm in two independent pre-clinical models of GBM that VB-111 significantly extends survival, inhibits tumor growth and decreases the volume of angiogenic vessels within the tumor. Given the data presented herein, coupled with human trials, we conclude that VB-111 displays efficacy as a new antiangiogenic agent for the treatment of glioblastoma.

Materials and Methods

Cell lines

Human glioma tumor cell lines U251-luc-RFP and U87MG-luc2 (Caliper LRS) were maintained as neurospheres in Neurobasal media (GIBCO) with supplements. Both glioma cell lines express firefly luciferase and RFP as tumor biomarkers. Prior to intracranial implantation, neurospheres were dispersed with accutase (MP Biomedicals) and resuspended to a final concentration of 2×10^5 cells per microliter.

Intracerebral xenograft models

One strain of nude rats (Athymic HsdHan: RNU-Foxn1rnu) and one strain of nude mice (Hsd:Athymic nude-Foxn1^{nu}) from Harlan labs were used for survival studies. The animals were anesthetized with isoflurane (2.5%) and stereotactically injected with 1×10^6 glioma cells into the right forebrain (rats: 4 mm lateral and 1 mm anterior to bregma, at a 4.5 mm depth from the skull surface; mice: 2mm, 2mm, 3 mm). Once tumors were established, groups of animals were randomized to respective treatment or control arms. All animal experiments were performed according to the National Institutes of Health Guide for the Care and Use of Experimental Animals protocol. Animals were sacrificed when moribund, listless, or when manifesting significant neurologic deficit.

Cranial window models

A cranial window was placed for visualization of tumor cells and associated brain vessels as follows: Athymic nude mice (Harlan Labs) were anesthetized and placed onto a stereotaxic stage and administered dexamethasone (0.02 ml at 4 mg/ml) and carprofen (4 mg/kg of a 50mg/ml solution) by intramuscular injection preoperatively. The scalp was retracted to expose the bregma and the periosteum was covered with lidocaine solution sufficiently to result in hemostasis during scraping. The periosteum was gently scraped with a scalpel to expose the cranium, and the surface dried. Using a high-speed micro-drill (0.5mm, Stoelting Co), the cranium was thinned in a circumference of a 5×5 mm region of the skull over the region of interest and the piece of bone was gently removed. 5 μl of suspension containing 1×10^6 U251 cells was stereotactically injected into the brain at a depth of 1 mm below the dura using 10 μl Hamilton microsyringe. A round cover slip (5–7 mm diameter, No. 1 thickness) was placed to cover the open-skull region and sealed with a thin layer of cyanoacrylate glue and dental acrylic. Similar supporting cranial window studies were conducted using TIE2-GFP transgenic mice which express GFP specifically in endothelial cells, whereby neovascular structures fluoresce. Placement of the cranial window thereby permits the visualization of GFP-positive blood vessels (data not shown).

Treatment protocol

VB-111 was provided by Vascular Biogenics (Or Yehuda, Israel), and was used directly and undiluted. Rats at 21 days post-implant or mice at 14 days post-implant were sedated with isoflurane to allow lateral tail vein injection of VB-111. A total dose of 2.5×10^{11} VPs in a volume of 250 μl was used for rats and 1×10^{11} VPs in a volume of 100 μl was used for mice.

Bioluminescence imaging

Tumor growth was monitored by luciferase imaging. Animals were anesthetized, injected with D-luciferin at 50 mg/ml i.p., and after 10 min imaged on an IVIS Lumina system. To quantify bioluminescence, regions of interest (ROI) were obtained utilizing an automated method by Living Image software (Caliper Life Science). Measurements over the course of the study were acquired weekly to track tumor growth dynamics.

Magnetic resonance imaging (MRI)

MRI was performed at days 0, 7, and 14 after VB-111 infusion on a Bruker Biospec 7-Tesla scanner (Bruker) as previously described [19]. Blood flow and blood volume were measured using dynamic contrast enhanced imaging following a bolus of gadopentetate-dimeglumine (GdDTPA). For dynamic contrast enhanced MRI, single-shot gradient echo planar imaging (EPI) was used, resolution of 0.27×0.27×0.5 mm, 5 slices (no gap), matrix = 96×96, field of view = 25.6×25.6 mm, repetition time TR = 0.5 s, echo time TE = 20 ms. For T1-weighted MRI, conventional acquisition was used, resolution of 0.27×0.27×0.5 mm, 15 slices (no gap), matrix = 96×96, field of view = 25.6×25.6 mm, repetition time TR = 0.5 s, echo time TE = 20 ms. The number of slices to cover the entire tumor region and roughly cover the entire cerebrum were selected.

Fluorescence microscopy

Temporal changes in the existing and newly formed brain vasculature were evaluated by fluorescence microscopy through a cranial window to track modulation in response to VB-111. To visualize the tumor-associated brain vessels in athymic nude mice (NU/J), we injected GFP-conjugated dye (FITC-dextran) into the tail vein to demarcate blood vessels. In contrast, the tumor cells (U251) were labeled with red fluorescent protein (RFP). Confocal images were captured with a Nikon Apo LWD 25X/NA1.1 water immersion objective on a Nikon Eclipse FN-1 microscope with a Prairie imaging system. Prairie View software was used for image collection. Excitation wavelength for GFP and RFP were 488 and 542 nm, respectively. Z-stacks of 180 single images with a 3-micron step and 512×512 pixel frame size were acquired. Images, color-coded green and red, for GFP and RFP, respectively, were subsequently merged into a single image. For each mouse, Z-stacks from four congruent and adjacent locations within the brain tumor area were obtained through the cranial window at week 1 (before treatment) and identical regions recorded at weeks 2, 3, 4, 5 and 6 (throughout and after treatment). Superficial blood vessel patterns were used as a guide to repeatedly image regions of interest. The microvascular density was defined as a ratio of the total fluorescence area (TFA) to the total area of an imaged field and was used as a surrogate measure of angiogenesis. Images from four different locations per mouse were collected for qualitative analysis.

Immunohistochemistry

Tissues were fixed in formalin, embedded in paraffin, and sectioned (5μm). After deparaffination, sections were stained for CD31 (SZ31; Dianova DIA-310) 1:10, and goat anti rat IgG-HRP (eBioscience 18-4818) 1:50. The capillary area was determined by

analyzing CD31-positive area using NIS Elements BR image analysis. In addition, the number of capillaries were counted per view of field (x100) (control n=9; VB-111 n=6).

Statistical analysis

Survival curves and statistical analysis were generated using GraphPad Prism 6 software. The program provides a Kaplan-Meier life-table analysis for each group (cumulative survival proportions with their 95% confidence intervals, median and mean survival times, and the incidence rate of the event), comparisons of survival proportions, tests comparing survival distributions (log rank and Gehan-Wilcoxon test), the ratio of median survival times and the hazard ratio (with 95% confidence intervals), and the trends in the early and later periods. Results were expressed as the mean ± SEM.

Results

Effect of VB-111 on the survival of intracranial glioma bearing rodents

As phase I/II clinical trials demonstrate that VB-111 is well tolerated and expressed in tumor tissue with some response, we sought to determine the efficacy of VB-111 in extending survival in animal models of GBM. Using two commercially available human GBM tumor cell lines (U87MG and U251) engineered to express firefly luciferase, we established intracranial GBMs into athymic nude rats and athymic nude mice to assess longevity, tumor growth and changes in blood vessels in the brain in response to VB-111 therapy. Before treatment with VB-111, animals were imaged using IVIS Imaging System for baseline determination of tumor size, then randomly assorted onto treatment (n=10) and control (n=9) arms. Vehicle control rats succumbed between day 34 and 49 post-implantation and demonstrated a median survival of 38 days (95% CI 35.1–40.9 days), which was commensurate with results seen from multiple prior experiments performed within our lab utilizing this model and cell line. Rats treated with VB-111 survived between 32 and 53 days and demonstrated a significant extension in survival to a median of 48 days (95% CI 42.1–53.9 days). Log rank analysis of survival distributions between these two groups showed a significant difference ($p<0.05$) in favor of treatment (Fig. 2A).

Experiments with athymic nude mice using the U251 cell line (n=20) also showed significant extension of survival after infusion of a single dose of VB-111 ($p<0.05$) (Fig. 2B). The median survival time of treated animals was increased by 13 days compared with the controls (median survival - 82 and 69 days; 95% CI - 74.1–96.1 and 60.4–78.0 days, respectively). A similar trend toward increased survival was also seen in separate experiments using U251-bearing mice which were fitted with cranial windows for imaging the tumor associated vasculature. Here the vehicle control mice demonstrated a median survival time of 45 days (95% CI 40–50 days), compared to VB-111 treated mice which survived to a median of 62 days (95% CI 60.78–63.22 days).

Quantitative assessment of tumor growth

Intracranial tumor growth was monitored using bioluminescence imaging on an IVIS Lumina system. Bioluminescence values were used as a surrogate marker for regression or growth of luciferase-expressing tumors. When tumors achieved detectable levels (21 and 14

days after tumor implantation for rats and mice, respectively) animals were imaged at weekly intervals immediately prior to and throughout and following treatment. At baseline, animals were randomized by ROI luciferase values into two weighted groups. Mean ROI luciferase intensities of U87MG tumor-bearing nude rats (n=20) began separating among the two groups at 1 week post treatment and continued thereafter (Fig. 3A). By week 4 the luciferase values were approximately two-fold higher in the control animals with a mean intensity of 4.9×10^6 while the VB-111 group showed a mean intensity of 2.4×10^6. This trend persisted through the 8 week study in which all animals eventually succumbed to their tumor burden after achieving a lethal level of 10^8.

In a supporting study, intracranial tumor growth was assessed in nude mice bearing U251 (n=20). No significant trend among groups was observed by IVIS imaging until week 10 of the 10 week study ($p<0.05$). Intriguingly, 3 of 10 mice demonstrated a complete response to VB-111 and were considered long term survivors. Of these, 2 responders segregated after only 1 week of treatment and the third animal responded after 5 weeks (data not shown). At the conclusion of this study, whole brains were removed and fixed for H&E staining to determine tumor size, which was defined as the ratio of the tumor area to the area of the whole brain. Here we found that VB-111 treated animals had a significantly smaller tumor compared to controls ($p<0.005$).

Correlation between bioluminescence and corresponding tumor volume

Because of the inherent limitations of measuring tumor volumes with bioluminescence, including the difficulty measuring necrotic core material and regions of hypoxia that may not permit proper oxidation of D-luciferin, we evaluated intracranial tumor growth in a subpopulation of nude rats bearing U87MG using MRI. Randomly selected animals were imaged at days 0, 7 and 14 relative to treatment. Although the sample size was inadequate to make a statistically significant comparison of tumor volumes among treatment groups, there was a clear trend toward decreased tumor volume post treatment with VB-111 compared to control. While control tumors had a more solid appearance with homogenous contrast enhancement typical for U87MG growth, those treated with VB-111 were more centrally necrotic appearing with a rim of enhancement (Fig. 3B). Perfusion imaging was difficult to interpret and showed no obvious trend with varying relative cerebral blood volume (rCBV) in control and treated tumors (data not shown). This may be due to mixed vascular disrupting and antiangiogenic effects of VB-111, which have offsetting effects on rCBV.

Antivascular effect of VB-111 in mouse models

To examine the antivascular effects of VB-111 on the tumor vessels of mice bearing GBM, we performed IHC staining with CD31, a common marker for quantifying tumor neovascularization. Terminal brain sections were prepared from U251 xenograft control (n=9) and VB-111 (n=6) treated mice and CD31 positive areas (μm^2) within control sections were 5-fold higher versus sections from VB-111 treated mice ($p=0.022$; Fig. 4A, 4B). Additionally the number of CD31 positive capillaries were counted per field of view and the mean number of microvessels in the VB-111 treatment group were three-fold lower compared to control ($p=0.003$; Fig. 4C). Given the inability to discern an effect on rCBV from VB-111, we assessed the qualitative changes in tumor-associated vasculature by direct

in-vivo fluorescence microscopy. Fluorescence microscopy through a cranial window allowed us to track the dynamic interactions occurring among the blood vessels and RFP-expressing U251 tumor in the exact same location of the brains over the course of 6 weeks. Two different animal models were used: 1) transgenic TIE2GFP mice with stable GFP expression in endothelial cells (data not shown), and 2) standard athymic nude mice administered FITC conjugated dextran into the tail vein (Fig. 5). We evaluated the ability of VB-111 to inhibit tumor-associated blood vasculature using a cranial window on athymic nude mice injected with FITC-dextran for labeling of total blood vessels (n=3). Treated mice (n=2) showed a maximum decrease of 23% vascular surface area by week 3 (Fig. 5B).

Discussion

In last decade, several antiangiogenic therapeutics have been evaluated for the treatment of glioblastoma [13, 20–22]. However, overall these studies have been underwhelming with minimal extension in survival even in the minority of patients who initially responded to treatment [13, 14]. While a number of potential resistance mechanisms may explain these shortcomings, reports provide evidence that solid tumors may upregulate VEGFR-independent pathways that preclude sensitivity to existing antiangiogenic drugs [23, 24]. Therefore, development of targeted gene therapy-based approaches, which are not pathway dependent, may provide broader activity and offer a greater survival benefit. VB-111, which is currently in phase I/II clinical trials is an adenoviral-based gene therapy that specifically targets the Fas-chimera transgene to newly formed angiogenic vessels to induce apoptosis.

In this report we present our pre-clinical findings concerning the efficacy of VB-111 in targeting angiogenic blood vessels and extending survival. Using two commercial GBM tumor cell lines, U87MG and U251, which recapitulate some features of the human GBM [25–27], we show that a single intravenous dose of VB-111 was sufficient to significantly prolong survival in athymic rats and mice. Median survival was observed to be extended by 10 and 12 days for U87MG and U-251 cell line, respectively, and log rank analysis confirms a statistically significant difference in favor of VB-111 ($p<0.05$). The improved survival seen with VB-111 compares favorably with existing anti-VEGF therapies tested in these models, both in our laboratory (data unpublished) as well as by others [28]. In fact, this impact on survival surpasses that of the VEGF-R inhibitor sunitinib (increase in median of 9 days) in the same model given for 5 days per week continuously [20].

Further, bioluminescent imaging of tumors in nude rats showed that tumor progression was delayed with a single dose of VB-111, with an approximate 2-fold decrease in median and mean luciferase activity at week 4 post inoculations. Although supporting MRI perfusion imaging was noncontributory, there may be multiple explanations for this. First, vascular disrupting agents (VDAs) we now know have an opposite effect on perfusion imaging compared to antiangiogenics with VDAs actually increasing perfusion in the tumor while antiangiogenic agents decrease perfusion [29]. Additionally, it has been suggested by some that dynamic susceptibility contrast imaging used may be inferior to dynamic contrast enhancement for evaluation of antiangiogenic agents and therefore was less ideal [30].

As tumor growth is supported by the formation of neovascular structures within and immediately surrounding the tumor, we next evaluated the effects of VB-111 on the number of new blood vessels found within the nude mouse brain tumor areas. Quantitative analysis of the total number of capillaries within the tumors of (n=9) control and (n=6) VB-111-treated nude mice suggests that microvessel density, as determined by CD31 staining, was significantly lower in the VB-111 treated group relative to control (p=0.003). Ongoing mechanistic studies that determine the precise signaling pathways leading to apoptosis of angiogenic tumor vasculature in response to VB-111 are of significant therapeutic value as this gene therapy was shown to be well tolerated in phase I clinical trials. Additional studies looking at the potential of VB-111 to target coopted normal vasculature within the tumor microenviroment are also of interest as these are known to play a significant role during tumorigenesis.

Based upon these pre-clinical findings, combined with our previous dose escalation, first-in-human trial of VB-111, we conclude that VB-111 displays efficacy as an antiangiogenic agent in the treatment of glioblastoma. Currently, VB-111 is in a phase II clinical trial in patients with recurrent antiangiogenic naïve glioblastoma.

Acknowledgments

Statement Detailing Funding: The study was supported by in part by the UTHSCSA Cancer Therapy and Research Center through the National Institutes of Health. National Cancer Institute P30 award CA054174, as well as by a service agreement with VBL Therapeutics.

Reference List

1. Wen PY, Kesari S. Malignant gliomas in adults. The New England journal of medicine. 2008; 359:492–507.10.1056/NEJMra0708126 [PubMed: 18669428]
2. Jain RK, di Tomaso E, Duda DG, Loeffler JS, Sorensen AG, Batchelor TT. Angiogenesis in brain tumours. Nature reviews Neuroscience. 2007; 8:610–622.10.1038/nrn2175 [PubMed: 17643088]
3. Carbone C, Campisi A, Musumeci T, Raciti G, Bonfanti R, Puglisi G. FA-loaded lipid drug delivery systems: preparation, characterization and biological studies. European journal of pharmaceutical sciences: official journal of the European Federation for Pharmaceutical Sciences. 2014; 52:12–20.10.1016/j.ejps.2013.10.003 [PubMed: 24514450]
4. Salameh TS, Banks WA. Delivery of therapeutic peptides and proteins to the CNS. Advances in pharmacology. 2014; 71:277–299.10.1016/bs.apha.2014.06.004 [PubMed: 25307220]
5. Garrido W, Rocha JD, Jaramillo C, Fernandez K, Oyarzun C, San Martin R, Quezada C. Chemoresistance in high-grade gliomas: relevance of adenosine signalling in stem-like cells of glioblastoma multiforme. Current drug targets. 2014; 15:931–942. [PubMed: 25174341]
6. Tentori L, Ricci-Vitiani L, Muzi A, Ciccarone F, Pelacchi F, Calabrese R, Runci D, Pallini R, Caiafa P, Graziani G. Pharmacological inhibition of poly(ADP-ribose) polymerase-1 modulates resistance of human glioblastoma stem cells to temozolomide. BMC cancer. 2014; 14:151.10.1186/1471-2407-14-151 [PubMed: 24593254]
7. Frampton JE, Keating GM. Bevacizumab: in first-line treatment of advanced and/or metastatic renal cell carcinoma. BioDrugs: clinical immunotherapeutics, biopharmaceuticals and gene therapy. 2008; 22:113–120.
8. Gubbi A, Kendrick JE, Finkler NJ. The role of bevacizumab in recurrent, platinum-sensitive ovarian cancer. Expert review of anticancer therapy. 2014; 14:1105–1113.10.1586/14737140.2014.956095 [PubMed: 25189201]
9. Keating GM. Bevacizumab: a review of its use in advanced cancer. Drugs. 2014; 74:1891–1925.10.1007/s40265-014-0302-9 [PubMed: 25315029]

10. Maillet M, Dreanic J, Dhooge M, Mir O, Brezault C, Goldwasser F, Chaussade S, Coriat R. The predictive and prognostic value of the Glasgow Prognostic Score in metastatic colorectal carcinoma patients receiving bevacizumab. Anti-cancer drugs. 2014; 25:1215–1219.10.1097/CAD.0000000000000129 [PubMed: 24858536]
11. Odia Y, Shih JH, Kreisl TN, Fine HA. Bevacizumab-related toxicities in the National Cancer Institute malignant glioma trial cohort. Journal of neuro-oncology. 2014; 120:431–440.10.1007/s11060-014-1571-6 [PubMed: 25098701]
12. Zinner RG, Obasaju CK, Spigel DR, Weaver RW, Beck JT, Waterhouse DM, Modiano MR, Hrinczenko B, Nikolinakos PG, Liu J, Koustenis AG, Winfree KB, Melemed SA, Guba SC, Ortuzar WI, Desaiah D, Treat JA, Govindan R, Ross HJ. PRONOUNCE: Randomized, Open-Label, Phase III Study of First-Line Pemetrexed + Carboplatin Followed by Maintenance Pemetrexed versus Paclitaxel + Carboplatin + Bevacizumab Followed by Maintenance Bevacizumab in Patients ith Advanced Nonsquamous Non-Small-Cell Lung Cancer. Journal of thoracic oncology: official publication of the International Association for the Study of Lung Cancer. 201410.1097/JTO.0000000000000366
13. Cea V, Sala C, Verpelli C. Antiangiogenic therapy for glioma. Journal of signal transduction. 2012; 2012:483040.10.1155/2012/483040 [PubMed: 22830012]
14. Hou LC, Veeravagu A, Hsu AR, Tse VC. Recurrent glioblastoma multiforme: a review of natural history and management options. Neurosurgical focus. 2006; 20:E5. [PubMed: 16709036]
15. Greenberger S, Shaish A, Varda-Bloom N, Levanon K, Breitbart E, Goldberg I, Barshack I, Hodish I, Yaacov N, Bangio L, Goncharov T, Wallach D, Harats D. Transcription-controlled gene therapy against tumor angiogenesis. The Journal of clinical investigation. 2004; 113:1017–1024.10.1172/JCI20007 [PubMed: 15057308]
16. Harats D, Kurihara H, Belloni P, Oakley H, Ziober A, Ackley D, Cain G, Kurihara Y, Lawn R, Sigal E. Targeting gene expression to the vascular wall in transgenic mice using the murine preproendothelin-1 promoter. The Journal of clinical investigation. 1995; 95:1335–1344.10.1172/JCI117784 [PubMed: 7883980]
17. Varda-Bloom N, Shaish A, Gonen A, Levanon K, Greenbereger S, Ferber S, Levkovitz H, Castel D, Goldberg I, Afek A, Kopolovitc Y, Harats D. Tissue-specific gene therapy directed to tumor angiogenesis. Gene therapy. 2001; 8:819–827.10.1038/sj.gt.3301472 [PubMed: 11423929]
18. Brenner AJ, Cohen YC, Breitbart E, Bangio L, Sarantopoulos J, Giles FJ, Borden EC, Harats D, Triozzi PL. Phase I dose-escalation study of VB-111, an antiangiogenic virotherapy, in patients with advanced solid tumors. Clinical cancer research: an official journal of the American Association for Cancer Research. 2013; 19:3996–4007.10.1158/1078-0432.CCR-12-2079 [PubMed: 23589178]
19. Phillips WT, Goins B, Bao A, Vargas D, Guttierez JE, Trevino A, Miller JR, Henry J, Zuniga R, Vecil G, Brenner AJ. Rhenium-186 liposomes as convection-enhanced nanoparticle brachytherapy for treatment of glioblastoma. Neuro-oncology. 2012; 14:416–425.10.1093/neuonc/nos060 [PubMed: 22427110]
20. de Bouard S, Herlin P, Christensen JG, Lemoisson E, Gauduchon P, Raymond E, Guillamo JS. Antiangiogenic and anti-invasive effects of sunitinib on experimental human glioblastoma. Neuro-oncology. 2007; 9:412–423.10.1215/15228517-2007-024 [PubMed: 17622648]
21. Furnari FB, Fenton T, Bachoo RM, Mukasa A, Stommel JM, Stegh A, Hahn WC, Ligon KL, Louis DN, Brennan C, Chin L, DePinho RA, Cavenee WK. Malignant astrocytic glioma: genetics, biology, and paths to treatment. Genes & development. 2007; 21:2683–2710.10.1101/gad.1596707 [PubMed: 17974913]
22. Soda Y, Myskiw C, Rommel A, Verma IM. Mechanisms of neovascularization and resistance to anti-angiogenic therapies in glioblastoma multiforme. Journal of molecular medicine. 2013; 91:439–448.10.1007/s00109-013-1019-z [PubMed: 23512266]
23. Baker GJ, Yadav VN, Motsch S, Koschmann C, Calinescu AA, Mineharu Y, Camelo-Piragua SI, Orringer D, Bannykh S, Nichols WS, deCarvalho AC, Mikkelsen T, Castro MG, Lowenstein PR. Mechanisms of glioma formation: iterative perivascular glioma growth and invasion leads to tumor progression, VEGF-independent vascularization, and resistance to antiangiogenic therapy. Neoplasia. 2014; 16:543–561.10.1016/j.neo.2014.06.003 [PubMed: 25117977]

24. Nandhu MS, Hu B, Cole SE, Erdreich-Epstein A, Rodriguez-Gil DJ, Viapiano MS. Novel paracrine modulation of Notch-DLL4 signaling by fibulin-3 promotes angiogenesis in high-grade gliomas. Cancer research. 2014; 74:5435–5448.10.1158/0008-5472.CAN-14-0685 [PubMed: 25139440]

25. Conrad C, Miller CR, Ji Y, Gomez-Manzano C, Bharara S, McMurray JS, Lang FF, Wong F, Sawaya R, Yung WK, Fueyo J. Delta24-hyCD adenovirus suppresses glioma growth in vivo by combining oncolysis and chemosensitization. Cancer gene therapy. 2005; 12:284–294.10.1038/sj.cgt.7700750 [PubMed: 15650766]

26. Jiang H, Gomez-Manzano C, Alemany R, Medrano D, Alonso M, Bekele BN, Lin E, Conrad CC, Yung WK, Fueyo J. Comparative effect of oncolytic adenoviruses with E1A-55 kDa or E1B-55 kDa deletions in malignant gliomas. Neoplasia. 2005; 7:48–56.10.1593/neo.04391 [PubMed: 15720816]

27. Samoto K, Ehtesham M, Perng GC, Hashizume K, Wechsler SL, Nesburn AB, Black KL, Yu JS. A herpes simplex virus type 1 mutant with gamma 34.5 and LAT deletions effectively oncolyses human U87 glioblastomas in nude mice. Neurosurgery. 2002; 50:599–605. discussion 605–596. [PubMed: 11841729]

28. Gomez-Manzano C, Holash J, Fueyo J, Xu J, Conrad CA, Aldape KD, de Groot JF, Bekele BN, Yung WK. VEGF Trap induces antiglioma effect at different stages of disease. Neuro-oncology. 2008; 10:940–945.10.1215/15228517-2008-061 [PubMed: 18708344]

29. Muldoon LL, Gahramanov S, Li X, Marshall DJ, Kraemer DF, Neuwelt EA. Dynamic magnetic resonance imaging assessment of vascular targeting agent effects in rat intracerebral tumor models. Neuro-oncology. 2011; 13:51–60.10.1093/neuonc/noq150 [PubMed: 21123368]

30. Provenzale JM. Imaging of angiogenesis: clinical techniques and novel imaging methods. AJR American journal of roentgenology. 2007; 188:11–23.10.2214/AJR.06.0280 [PubMed: 17179341]

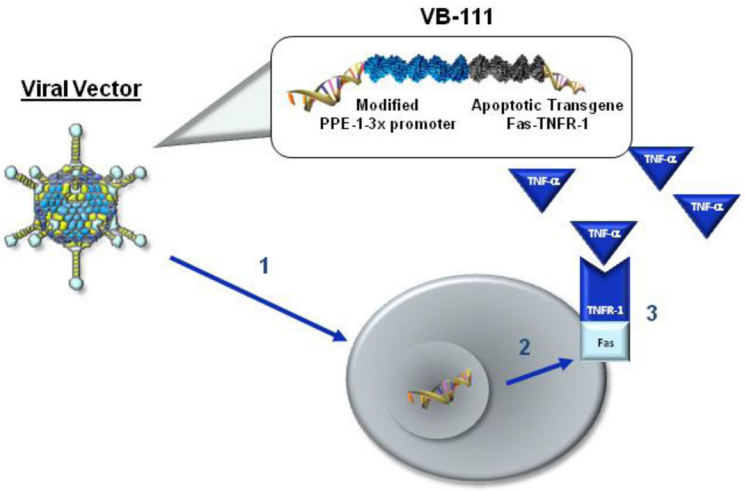

Figure 1.

Mechanism of action of VB-111. (1) Viral vector internalized into endothelial cells in angiogenic blood vessels. (2) PPE-1-3x promoter causes Fas-TNFR-1 to be expressed on the endothelial cell surface. (3) Cell apoptosis is activated when circulating TNF-α interacts with Fas-TNFR-1 receptor.

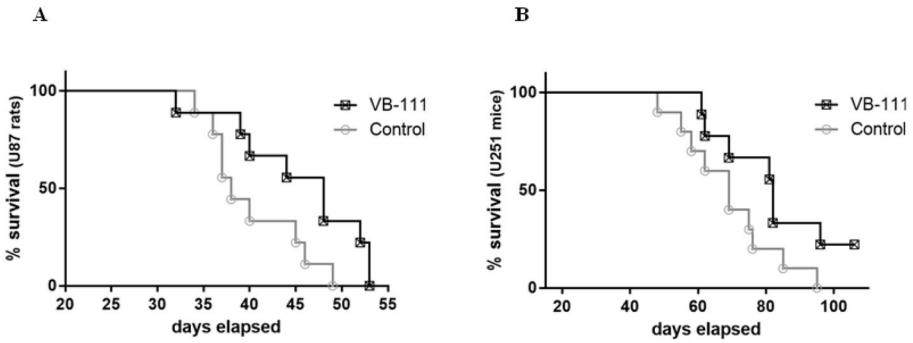

Figure 2.

Survival of control and treated athymic nude rats and mice after a single dose of VB-111. (A) Nude rats bearing U87MG (9 control and 10 treated rats). (B) Nude mice bearing U251 (10 mice for each group). Survival distributions for both xenograft models showed a significant difference ($p<0.05$) in favor of treatment with a 10 day increase in median survival in the VB-111 treated rats and a 13 day increase in the VB-111 treated mice versus respective control.

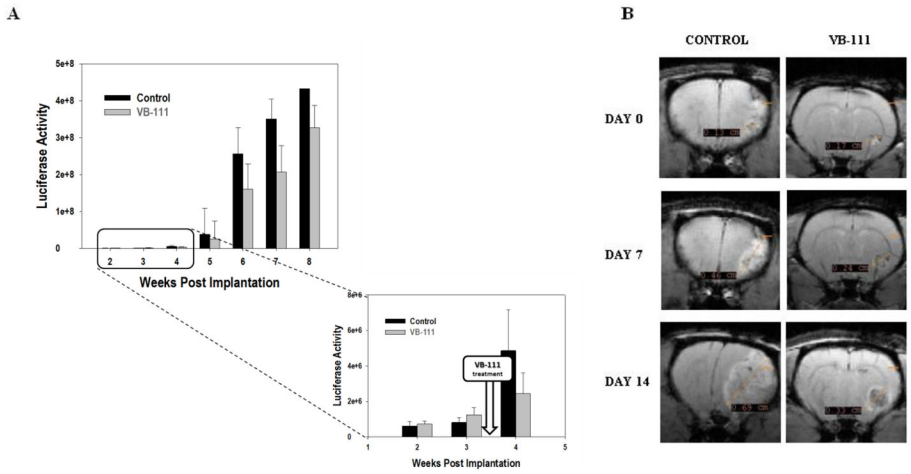

Figure 3.

(A) Luciferase emission quantification as a surrogate for tumor volume from nude rats bearing U87MG xenografts (10 animals per group). At week 4 luciferase values separated among the two groups. (B) Representative examples of MRI of treated and control U-87MG bearing rats before (day 0) and after VB-111 treatment (day 7, day 14). The control shows homogenous contrast enhancement, is more solid appearing, and is associated with marked mass effect and midline shift. By contrast, the treated tumor displays central necrosis, minimal mass effect, and a rim of enhancement.

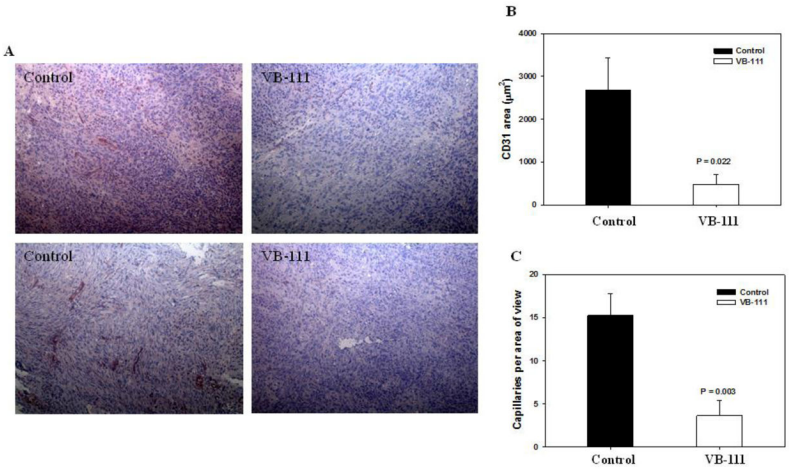

Figure 4.

Immunohistochemical evaluation of the effect of VB-111 on the intratumoral vasculature within established U251 xenografts (9 control and 6 treated nude mice). Quantitative analysis shows a significant decrease in microvessel density (CD31) in VB-111 treated group relative to control group. (A) Representative examples for the detection of CD31 in tumor sections from the control and VB-111 treatment groups (4X). (B) Quantitative comparison of CD31-positive areas of the tumor sections from two groups of animals (p=0.022). (C) The total number of capillaries were counted per field of view at x100 magnification (p=0.003).

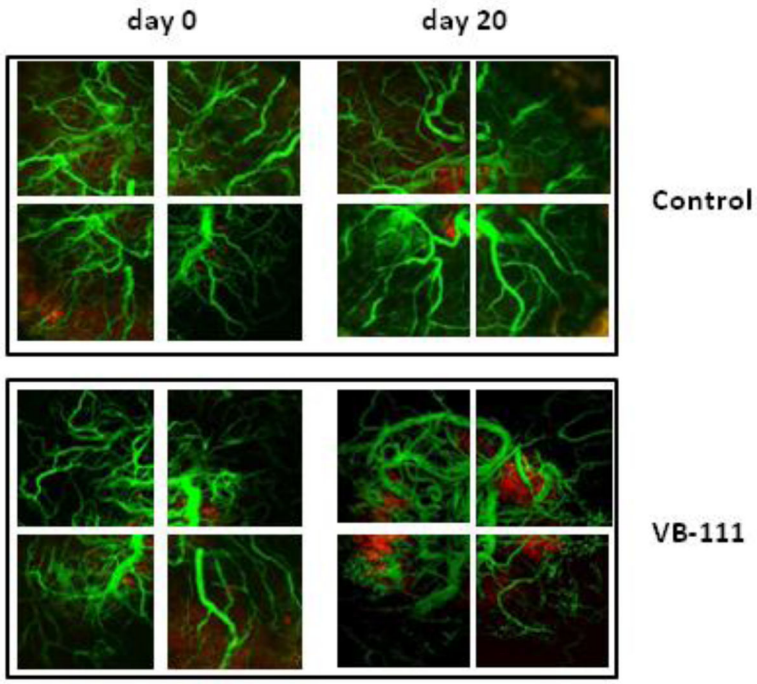

Figure 5.

In vivo images of the intracranial tumor-associated vasculature were acquired by confocal microscopy at day 0 (left column) and day 20 (right column) with control (top panel) or VB-111 treatment (bottom panel). These standard athymic nude mice (n=3) were injected with FITC conjugated dextran (green) to determine the effects of VB-111 on the tumor-associated vessel density. A single dose of VB-111 leads to the continuous reduction in the density of blood vessels in the tumor area (red) in transgenic mice bearing U251 cells.